Macromolecules

Perspective

pubs.acs.org/Macromolecules

Theory of Block Polymer Micelles: Recent Advances and Current Challenges

E. B. Zhulina[†] and O. V. Borisov*[,†,‡]

[†]Institute of Macromolecular Compounds, Russian Academy of Sciences, St. Petersburg 199004, Russia

[‡]Institut Pluridisciplinaire de Recherche sur l'Environnement et les Matériaux, UMR 5254, UPPA CNRS, 64053 Pau, France

ABSTRACT: We present an overview of existing theories of block polymer micelles. We focus here on the equilibrium structure of nanoaggregates formed by solvophobic/solvophilic diblock copolymers in a dilute solution and briefly address the association behavior of triblock terpolymer. We outline recent advances in the field and some challenging problems for theoretical developments.

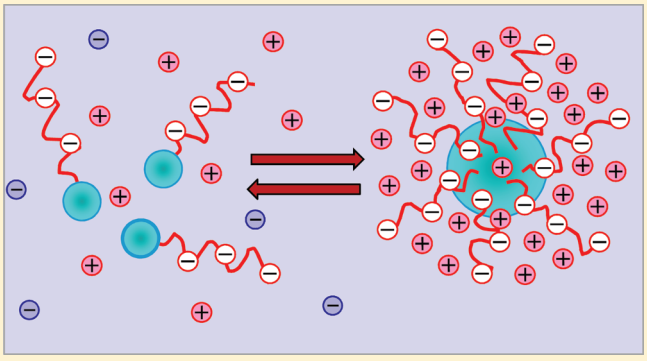

1. INTRODUCTION

In the past two decades a significant progress has been achieved in understanding self-assembly of block copolymers in selective solvents.[1,2] Association of the insoluble blocks of macromolecules gives rise to multichain aggregates whose thermodynamic stability in the solution is ensured by the soluble blocks. The copolymer topology, length, and solubility of the blocks specify the shape and the size of assembling aggregates. A typical example is a spherical micelle formed by diblock *AB* copolymer in a selective solvent. In such an aggregate, the micellar core composed of insoluble blocks *B* is surrounded by the corona of blocks *A* swollen in solvent *S*, and the core−corona interface is narrow compared to the sizes of core and coronal domains.

In this Perspective we highlight current state (state-of-the-art) of the theory of polymer micelles with focus on recent advances and current challenges. We primarily discuss here the theory of micelles formed by solvophobic/solvophilic diblock copolymer in a dilute solution and only briefly address the structures formed by triblock terpolymers.

Theoretical modeling of polymer micelles has progressed with the self-consistent field (SCF) methods.[3−11] The numerical SCF approach incorporates Edward's formalism[12] to account for chain conformations and takes advantage of the mean-field Flory−Huggins theory of polymer solutions.[13] The SCF models provided numerical dependences of the aggregation number and sizes of the core and coronal domains in an equilibrium micelle as a function of the degree of polymerization of the blocks, N_A and N_B, and the polymer−polymer and polymer−solvent Flory−Huggins interaction parameters, χ_{AB}, χ_{AS}, and χ_{BS}. This approach predicted the trends in a polymer micelle behavior and supported the narrow interface approximation which has been widely used in subsequent theoretical modeling. The numerical SCF methods were later extended to the case of charged block copolymers[14−16] and remain an important tool in the theoretical studies of polymer self-assembly.

Subsequent advances in the theory of polymer micelles were promoted by the scaling theory of polymer solutions.[17] In contrast to a mean-field Flory−Huggins theory, the scaling model accounted for the polymer density correlations and introduced the concept of correlation blob as an effective unit of a semidilute solution. A solution of flexible polymer chains with concentration c of monomer units is envisioned as a densely packed system of the correlation blobs with size $\xi(c)$ and the interaction free energy $\simeq k_BT$ per blob where k_B is the Boltzmann constant and T is the temperature. (Here and below, the symbol "$\simeq$" indicates the equality with accuracy of a numerical coefficient.) The dependence $\xi(c)$ is specified by the solvent quality as $\xi \sim c^{-\nu/(3\nu-1)}$ where exponent $\nu = 1/2$ and $\nu \approx 3/5$ under theta and good solvent conditions, respectively. Inside the correlation blob, the structure of a polymer chain is almost unperturbed by the interactions with neighboring chains, whereas at length scales much larger than $\xi(c)$, the interactions between distal parts of the chain are screened by other chains. As a result, each macromolecule is transformed into a Gaussian chain of $n(c)$ blobs with the average size $\simeq \xi(c)[n(c)]^{1/2}$, whereas the interaction free energy per chain is related to number $n(c)$ of the correlation blobs as $\simeq k_BTn(c)$.

Solutions of semiflexible polymers exhibit a more complex behavior. In addition to the scaling regime of semidilute solution (with dense packing of the correlation blobs under good solvent conditions), the theory[18,19] predicts an intermediate (mean-field) regime in a marginal good solvent. Here, the

Received: January 25, 2012
Revised: April 1, 2012

   dx.doi.org/10.1021/ma300195n | *Macromolecules* XXXX, XXX, XXX−XXX

mean-field exponents in power law dependences for the solution properties are recovered.

Below, we focus on flexible macromolecules with Kuhn segment length on the order of monomer size and briefly review the ideas that lead to first scaling models of diblock copolymer micelles.[20−23]

2. NONIONIC DIBLOCK COPOLYMER MICELLES

A narrow core−corona interface suggests that micellar corona can be envisioned as a polymer brush of soluble blocks *A*. The theory of polymer brushes started with the seminal works of Alexander[24] and de Gennes.[25] These studies laid a foundation for the scaling models of spherical[26,27] and cylindrical[27] brushes that mimic the coronal domains in nonplanar aggregates of diblock copolymers. The polymer density profile in a concave polymer brush (micellar corona) decays to the brush periphery, and thereby blob size ξ becomes dependent on distance r from the center of micelle. The condition of dense packing of the correlation blobs determines the blob size $\xi(r)$ for a given brush geometry and grafting density of the chains. The brush free energy is then calculated as total number of blobs times thermal energy k_BT.

With these ingredients, formulation of the free energy per chain F_{chain} in a diblock copolymer aggregate is straightforward. Three generic geometries i are considered (i = 1, 2, and 3 for lamellas, cylinders, and spheres, respectively; see Figure 1).

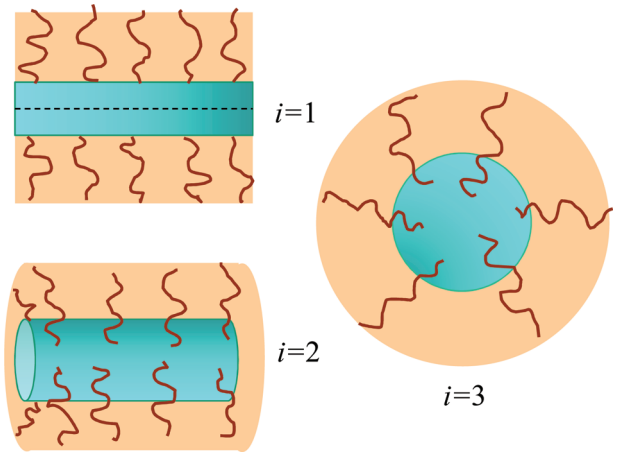

Figure 1. Schematic of three generic morphologies of self-assembled diblock copolymers: lamella (i = 1), cylindrical aggregate (i = 2), and spherical micelle (i = 3).

Following de Gennes,[20] the free energy per chain F_{chain} is represented as a sum of three contributions

$$F_{chain} = F_{interface} + F_B + F_A \quad (1)$$

Here

$$F_{interface} = \gamma s \quad (2)$$

where s is area per chain and γ is the free energy per unit area of the core−corona interface. Since the concentration of monomer units *A* at the core−corona interface is relatively small, the value of γ is controlled primarily by *B*−*S* interactions (specified by the Flory−Huggins interaction parameter χ_{BS}), and $\gamma \approx \gamma_{BS}$. F_B and F_A are the contributions due to blocks *B* and *A* in the coral and coronal domains of micelle, respectively.

The coral contribution $F_B = F_{B,interaction} + F_{B,elastic}$ comprises the free energy of interaction between monomers and the elastic free energy of extended blocks *B*. The polymer density distribution in the core of micelle formed by copolymer with relatively long blocks (N_A, $N_B \gg 1$) is almost uniform with volume fraction $\varphi_B \lesssim 1$. To a good approximation, φ_B coincides with that in a precipitate of polymer *B* in poor solvent *S*. Although free energy $F_{B,interaction} \sim k_BTN_B$ constitutes the largest contribution to F_{chain}, it does not depend on the core size or shape and is omitted from consideration. The free energy $F_{B,elastic}$ is approximated as

$$\frac{F_{B,elastic}}{k_BT} \approx b_i\frac{R^2}{a^2N_B} \quad (3)$$

where $R = iN_Ba^3/(\varphi_B s)$ is radius of the core, a is the size of monomer unit (for simplicity, sizes of monomer units *A* and *B* are assumed to be equal), and b_i is the geometry-dependent numerical coefficient. The values of $b_1 = \pi^2/8$, $b_2 = \pi^2/16$, and $b_3 = 3\pi^2/80$ were calculated in the seminal study of Semenov[28] in the limit when blocks *B* are noticeably extended with respect to Gaussian size, i.e., when $R > a(N_B)^{1/2}$.

The coronal contribution F_A is the free energy per chain in the brush formed by blocks *A*. The latter are "tethered" with grafting area s to the surface of micellar core with radius R (see Figure 2). Dense packing of blobs inside the corona prompts

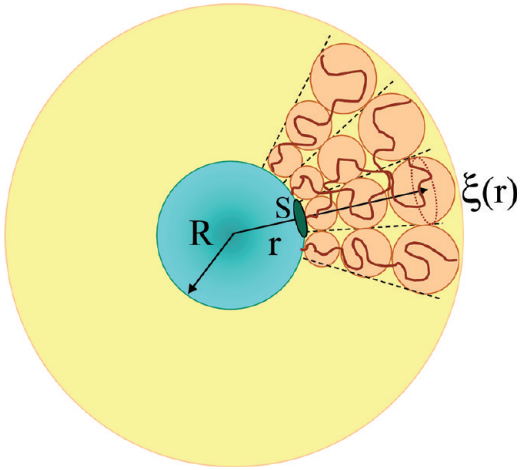

Figure 2. Schematic of blob structure of the coronal domain in a nonionic micelle.

that the blob size $\xi(r)$ increases with distance r from the center of micelle as

$$\xi(r) = \xi(R)\left(\frac{r}{R}\right)^{(i-1)/2} \simeq \sqrt{s}\left(\frac{r}{R}\right)^{(i-1)/2} \quad (4)$$

provided that the free ends of blocks *A* are localized within the outermost coronal blobs. The volume fraction $\varphi_A(r)$ of monomers *A* at distance r from the center of micelle is related to $\xi(r)$ as in a semidiliute polymer solution, $\xi(r) \simeq a\varphi_A(r)^{-\nu/(3\nu-1)}$. The latter relationship and eq 4 specify density profile $\varphi_A(r)$ in the micellar corona of geometry i. The scaling expression for coronal thickness H_i follows from the conservation condition

$$\int_R^{H_i+R} \varphi_A(r)\left(\frac{r}{R}\right)^{i-1} dr = \frac{N_A a^3}{s}$$

dx.doi.org/10.1021/ma300195n | Macromolecules XXXX, XXX, XXX−XXX

Free energy F_A (number of blobs per coronal block) is given by

$$\frac{F_A}{k_BT} = \int_R^{H_i+R} \frac{dr}{\xi(r)} \simeq \begin{cases} (R/\sqrt{s})\ln(1 + H_3/R) & i = 3 \\ 2(R/\sqrt{s})[(1 + H_2/R)^{1/2} - 1] & i = 2 \\ H_1/\sqrt{s} & i = 1 \end{cases} \quad (5)$$

Balance of the dominant contributions to the chain free energy, $F_{chain} \approx F_{interface} + F_A$, provides the equilibrium parameters of diblock copolymer aggregates: surface area s and sizes H_i and R of the coronal and core domains. The aggregates are characterized by total number of chains (aggregation number) $p \simeq R^2/s$ in a spherical micelle ($i = 3$), by number of chains per unit length (linear density) $\simeq R/s$ in a cylindrical aggregate ($i = 2$), and by number of chains per unit area of A/B interface (surface density) $1/s$ in a lamella ($i = 1$).

Division into starlike and crew-cut micelles allows for asymptotic dependences for micelle parameters in these two limits. Equation 5 indicates that when $H_i/R \gg 1$, the free energy of a spherical corona ($i = 3$) is much smaller than that in a cylindrical or planar coronae. Therefore, starlike micelles are always thermodynamically stable with respect to cylindrical and lamellar aggregates with large coronal domains. The aggregation number in an equilibrium starlike spherical micelle

$$p \simeq N_B^{4/5}\left(\frac{a^2\gamma_{BS}}{k_BT}\right)^{6/5} \quad (6)$$

is controlled primarily by the degree of polymerization N_B of insoluble block and only weakly (logarithmically) decreases with increasing length of coronal block A. Similarly to the numerical coefficient, the logarithmic prefactor in eq 6 is omitted.

In the opposite limit of crew-cut aggregates, expansion of F_A in eq 5 with respect to small parameter $H_i/R \ll 1$, with the account of curvature dependence of H_i gives[30]

$$\frac{F_A}{k_BT} \approx \frac{F_1 + \Delta F_A}{k_BT} \simeq \frac{H_1}{\sqrt{s}} - \frac{(i-1)}{4\nu}\frac{H_1^2}{R\sqrt{s}} \quad (7)$$

As it follows from eq 7, the coronal free energy F_A in crew-cut aggregate of morphology i has planarlike term $F_1(s)$ supplemented by the geometry-dependent correction (the second term in eq 7). Therefore, the dominant contribution to the chain free energy, $F_{chain} \approx F_{interface} + F_1$, is the same for $i = 1$, 2, and 3, and the crew-cut aggregates of all geometries exhibit universal power law dependence for area per chain s. In particular, for the spherical crew-cut micelles this leads to the scaling expression of aggregation number

$$p \simeq N_B^2\left(\frac{a^2\gamma_{BS}}{N_A k_BT}\right)^{6\nu/(2\nu+1)} \quad (8)$$

with remarkably stronger (power law) dependence on length N_A of the coronal block than in the case of starlike micelles (eq 6).

The difference δF_i in the free energies of crew-cut aggregates of various morphologies is attributed to the curvature induced correction ΔF_A and the elastic contribution $F_{B,elastic}$.[29] An increase in curvature of micellar core leads to the decrease in coronal free energy F_A (blocks A become less crowded, $\Delta F_A < 0$) with the simultaneous increase in conformational restrictions on the core blocks (blocks B become more elongated). Although in an equilibrium aggregate $F_{B,elastic}$ is always smaller than the surface free energy $F_{interface}$, it is *the elastic stretching of coral blocks B* that gives rise to *micelle polymorphism*. Without this contribution, an equilibrium diblock copolymer micelle would always have a spherical shape. The equilibrium morphology i of a crew-cut aggregate is dictated by the minimal free energy increment, $\delta F_i = F_{B,elastic} + \Delta F_A$. The condition $\delta F_i = \delta F_{i-1}$ determines the coexistence line (binodal) for morphological transformation $i \rightarrow i - 1$ ($i = 2, 3$).

The critical micelle concentration (CMC) for micelles of nonionic block copolymer is evaluated as

$$\ln \mathrm{CMC}_n \approx -F_{interface}(p = 1)/k_BT \quad (9)$$

Here, the subscript "n" indicates nonionic micelle, $F_{interface}(p = 1)$ is the surface free energy associated with a single condensed block B in a unimer, and the contribution of coronal blocks A is omitted. A more detailed discussion of the thermodynamics of micellization can be found in the review.[30]

Although the scaling model outlined above accounts only for the dominant power law dependences and neglects the numerical coefficients, it turned out to be a useful tool to analyze the experimental data on diblock copolymer micelles. Depending on the nature of coral block B, polymer micelles could be thermodynamically equilibrated or "frozen". Equilibrium conditions imply the exchange between polymer molecules in aggregates and unimers. In "frozen" aggregates this exchange is arrested, and such micelles are similar to starlike or comblike polymers with chemically fixed density of the branches. Some experimental systems have demonstrated reasonable agreement with the predicted scaling exponents (see, e.g., discussion in ref 23); in other studies[31,32] deviations between apparent and theoretical exponents were significant. A systematic analysis of scaling dependences of aggregation number p and the hydrodynamic radius of micelles formed by diblock copolymer poly(styrene)-*b*-poly(4-vinylpyridine) in selective solvent toluene has been performed in ref 33. It was demonstrated that while the hydrodynamic radius follows the theoretical predictions for starlike micelles, the value of exponent in the dependence of aggregation number p on length of coral block N_B is close to that predicted for crew-cut micelles. The observed dependence of aggregation number p on length of coronal block N_A was stronger than that predicted for starlike micelles (eq 6) but noticeably weaker than that given by eq 8 for crew-cut micelles. Noticeable discrepancies between the predicted and apparent values of exponents are typically attributed to the lack of full thermodynamic equilibration, sample polydispersity, choice of the system parameters in crossover region between the starlike and crew-cut regimes, etc.

Subsequent refinements to the scaling theory of nonionic block polymer micelles were performed along the following lines:

(i) Power law asymptotic dependences for micelle parameters are valid in the limits $H_i/R \gg 1$ (starlike aggregates) and $H_i/R \ll 1$ (crew-cut aggregates). However, the majority of experimental systems are found in the intermediate regime between these two limits. In order to make a comprehensive comparison between theory and experiment, it is therefore necessary to retain all the terms in F_A including the logarithmic dependence, eq 5, and also account for $F_{B,elastic}$ in minimizing the chain free energy F_{chain}. Such theoretical development[29] allowed for the analysis of discrepancies between full and

dx.doi.org/10.1021/ma300195n | *Macromolecules* XXXX, XXX, XXX−XXX

asymptotic expressions for aggregation number p and other micelle parameters.

(ii) A scaling model with specified values of b_i has two still unknown numerical coefficients. These coefficients may be introduced as prefactors in the dependences of thickness H_1 and free energy $F_1$of a planar brush.[29] They can be determined from fitting the experimental data on the spherical micelles (with $N_A \gtrsim N_B$) and later used for arbitrary values of N_A and N_B and different aggregate morphologies i.

(iii) A scaling theory with unspecified numerical coefficients is capable to predict polymorphism of crew-cut diblock copolymer micelles and to provide the values of exponents in power law dependences of the binodals. In particular, the model predicts that degrees of polymerization of coral block B, N_B^{s-c} and N_B^{c-l}, corresponding to respective sphere-to-cylinder and cylinder-to-lamella transitions, exhibit power law asymptotic dependences with similar values of exponents

$$N_B^{s-c} \simeq N_B^{c-l} \simeq \left(\frac{a^2\gamma_{BS}}{k_BT}\right)^{(2-7\nu)/(2+4\nu)} N_A^{11\nu/(2+4\nu)} \tag{10}$$

Numerical coefficients b_i permit to estimate the relative width $\Delta N_B/N_B^{c-l}$ of the corridor of thermodynamic stability of cylindrical micelles. Implementation of the full set of numerical coefficients allows for precise positions of the binodals in the N_A, N_B parameter space and direct comparison with the experiment. In Figure 3, we demonstrate the diagram of states

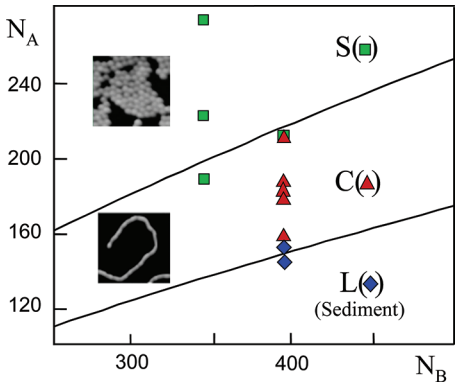

Figure 3. Diagram of states for nonionic block copolymer poly(styrene)-*b*-poly(isoprene) in *n*-heptane in N_A, N_B coordinates. Insets demonstrate AFM images of spherical and cylindrical micelles kindly provided by S. S. Sheiko.

in N_A, N_B coordinates of diblock copolymer poly(styrene)-*b*-poly(isoprene) in *n*-heptane. The binodals separating regions of thermodynamic stability of spherical (S), cylindrical (C), and lamellar (L) aggregates (shown by solid lines) were calculated using the full set of numerical coefficients obtained as explained above.[29]

(iv) Dense packing ansaz of the correlation blobs in micellar corona (Figure 2) is traceable to the Daoud–Cotton model of starlike polymers.[26] A more recent analysis[34] has demonstrated that such structure of a concave brush is not truly equilibrium. A lower free energy is attained when the chains stretch additionally to decrease monomer–monomer interactions at the brush periphery, thereby making blob arrangement more loose than dense packing. Although the effect is maximal in a starlike corona of spherical micelle, the values of exponents predicted by the original scaling model are unchanged while the decrease in the coronal free energy amounts to $\lesssim$10%. Remarkably, eq 7 is not affected and positions of the binodals for sphere-to-cylinder and cylinder-to-lamella transitions are not changed.

To conclude this section, we briefly outline few unsolved problems in the theory of nonionic polymer micelles:

- The effect of solvent properties on micellar structure is typically accounted through the values of Flory–Huggins interaction parameters χ_{BS} and χ_{AS} for monomer units of core and corona forming blocks. In experiment, mixtures of low molecular weight solvents are often used in micelle preparation protocol. The properties of a binary mixture of compatible solvents are well described through an effective (composition-dependent) Flory–Huggins interaction parameter.[35,36] However, for incompatible solvents, admixture of a thermodynamically better solvent could lead to a dramatic rearrangement in a brushlike corona. Abrupt collapse and reswelling were predicted to occur in a planar brush in contact with mixed solvents.[37,38] The collapse is accompanied by vertical brush segregation in two distinctive sublayers, each enriched in one of the solvents. Similar effects are possible in a concave corona of micelle in contact with mixed solvents that are equally poor for block B. Preferential solvation of the copolymer components by immiscible solvents could lead to even more complicated solvent distribution within a micelle.[39,40] However, up to now, the effects related to solvent complexity (including different solubilities of the components in solvent/cosolvent mixtures) remain essentially unaddressed in the analytical theory of polymer micelles.
- The models outlined in this section are applicable to copolymers with organo-soluble blocks (e.g., poly(styrene)-*b*-poly(isoprene) in *n*-heptane) or nonionic copolymers with water-soluble block (e.g., poly(ethylene oxide)) in the temperature interval distant from LSCT or UCST. Copolymers whose constituent blocks are flexible nonionic biopolymers (polypeptides)[41−43] could also form stable spherical micelles or cylindrical aggregates in an interval of temperatures. Thermoresponsive polypeptide blocks might exhibit elements of the secondary structure and undergo intramolecular conformational transitions (see schematic in Figure 4). Theoretical modeling of helix–coil transition in tethered polypeptides has been recently performed for planar brushes.[44] However,

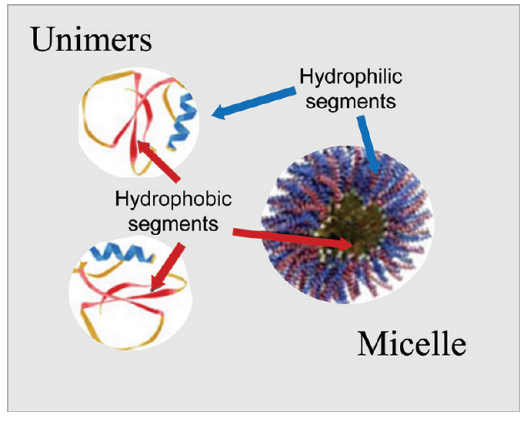

Figure 4. Schematic of polypeptide micelle.

dx.doi.org/10.1021/ma300195n | *Macromolecules* XXXX, XXX, XXX–XXX

incorporation of full conformational complexity of the components remains one of the challenging problems in the theory of diblock copolymer micelles.

- The theories of nonionic micelles focus mostly on the aggregates wherein core domain is in the elastomeric (amorphous) state. A number of experiments indicate that linear[45−49] and branched[50] block polymers with crystallizable insoluble block B could give rise to self-assembled aggregates with tunable morphology. The existing theoretical developments for such structures are limited.[51,52] A consistent calculation of the crystallization induced conformational entropy loss for block B could extend the theory of morphological transitions developed for micelles with elastomeric core to copolymer aggregates with crystallizable coral domain.

3. IONIC DIBLOCK COPOLYMER MICELLES

Similarly to nonionic macromolecules, diblock copolymers with hydrophobic and polyelectrolyte (PE) blocks give rise to a variety of nanostructures.[53] The interplay of long-range electrostatic interactions and van der Waals forces makes the behavior of charged amphiphilic macromolecules more complex compared to that of nonionic polymers.[54,55]

Self-assembled aggregates of block copolymer with weak (annealing) and strong (quenched) PE coronal blocks could demonstrate quite different features. In a corona composed of weak PE (e.g., poly(acrylic acid)), the fraction of charged monomers α is governed by the local (coronal) pH and can be tuned by variations in the ionic strength and pH in the solution. In a strong PE coronal block (e.g., sulfonated poly(styrene)), α is fixed chemically by the degree of chain sulfonation and does not depend on the environmental conditions. Both types of micelles are stimuli-responsive. That is, the size and shape of aggregates can be manipulated by tuning the strength of electrostatic interactions by, e.g., additions of salt ions or (in case of weak PE coronal block) by changing pH. We focus here on the conditions when ionization of PE block is lower than the Manning condensation threshold,[56] $\alpha l_B/a < 1$, where $l_B = e^2/\varepsilon k_B T$ is the Bjerrum length, e is elementary charge, ε is the dielectric constant, and $k_B T$ is the thermal energy. Under these conditions counterions retain the translational mobility within micellar corona and do not condense on ionized blocks A (see review[57] for a more detailed discussion).

Up to now, there is no analytical theory of a micelle with charged corona developed to the level of accuracy achieved for a neutral system. A recent review[30] summarizes the theoretical concepts and existing models of diblock copolymer micelles with ionized corona. The free energy per chain in such a micelle can be expressed by eq 1 with the coronal free energy

$$F_A = F_{ev} + F_{ion} \tag{11}$$

comprising the contributions due to both excluded volume (F_{ev}) and electrostatic (ionic) interactions (F_{ion}). The latter leads to additional extension of ionized blocks and violation of dense packing of the coronal correlation blobs. Similar to association of nonionic macromolecules, the equilibrium self-assembly of copolymer with ionizable coronal block is governed by the balance of the surface and the coronal free energies, $F_{interface} \simeq F_A$. The surface contribution $F_{interface}$ is almost unaffected by the presence of ionic groups and is still given by eq 2 with $\gamma \approx \gamma_{BS}$.

A consistent analytical theory of micelle with PE corona in contact with solution of salt requires the Poisson−Boltzmann approach to determine spacial distributions of electrostatic potential Ψ and of mobile ions in different geometries (spherical, cylindrical, and planar). This problem has been solved analytically for a planar PE brush that mimics the corona of a lamella ($i = 1$) in contact with solution of monovalent salt.[58−60] The dimensionless electrostatic potential $e\Psi/k_B T$ inside (negatively) charged planar corona of strong PE blocks A has a parabolic shape[58]

$$\frac{e\Psi(x)}{k_B T} = -\frac{H_1^2 - x^2}{H_0^2} \tag{12}$$

where H_1 is the coronal thickness, x is the distance from A/B interface, and $H_0 = a[8\alpha/(3\pi^2)]^{1/2} N_A$ is the characteristic electrostatic length. Electrostatic potential outside the corona coincides with that of a planar surface with charge number density $H_1/(2\pi l_B H_0^2)$. The thickness H_1 of the planar corona depends on salt concentration c_s in the solution (and on the molecular parameters of diblock copolymer), but the parabolic shape of $\Psi(x)$ (eq 12) remains unchanged upon additions of salt ions. For other geometries of ionized corona ($i = 2, 3$) the Poisson−Boltzmann equation for electrostatic potential $\Psi(x)$ could be solved numerically.

The numerical SCF models using Poisson−Boltzmann framework to treat electrostatic interactions[14,61] highlighted many details of the internal micelle organization. The analysis of ion distributions in micelle vicinity indicated that in salt-free solutions of charged micelles with aggregation number $p \gtrsim 10$ mobile ions are preferentially localized within coronal domain and almost fully compensate the "bare" charge $\alpha p N_A$ of the coronal blocks. Pioneering theoretical studies[62,63] established the difference between the two states of ionized coronal domain: with "bare" Coulomb repulsions between charged monomers and with counterions condensed in micellar corona. Subsequent studies concentrated mostly on micelles with ions localized in micellar corona and almost fully neutralized net coronal charge.

Below we focus on experimentally relevant case of aggregates with compensated coronal charge (see schematic in Figure 5).

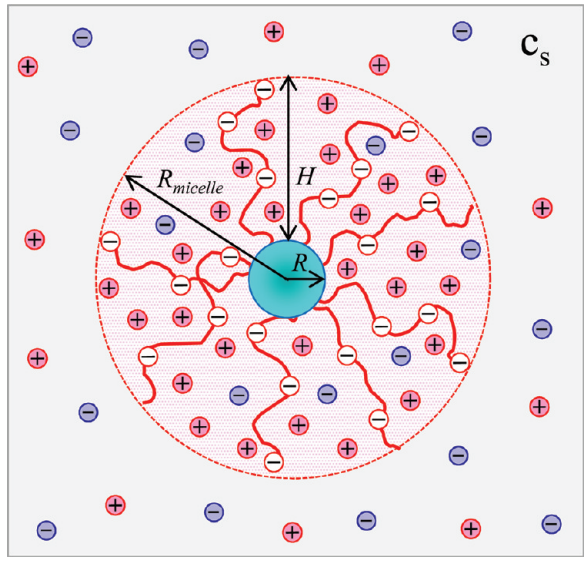

Figure 5. Schematic of spherical micelle with ionized corona in contact with solution of monovalent salt.

dx.doi.org/10.1021/ma300195n | *Macromolecules* XXXX, XXX, XXX−XXX

The coronae of such micelles is envisioned as totally and locally electroneutral polymer brush with entrapped mobile ions. The local electroneutrality approximation (LEA) assumes that the local number density of ionized monomers in a (negatively) charged corona of micelle is approximately equal to local excess number density of mobile counterions

$$\sum_{j^-} c_{j^-}(r) + \alpha(r)c_p(r) \approx \sum_{j^+} c_{j^+}(r) \tag{13}$$

Here, $c_j(r)$ is the local concentration of (monovalent) ions of type j, and $c_p(r)$ and $\alpha(r)$ are the concentration of the monomer units and the degree of ionization in the corona at a distance r from the center of micelle, respectively. The summation on the right-hand side of eq 13 includes all the cationic species (i.e., salt ions, c_{Na^+}, and hydrogen ions, c_{H^+}), whereas the summation on the left-hand side of eq 13 includes all the anionic species (i.e., salt ions, c_{Cl^-}, and hydroxyl ions, c_{OH^-}). The concentrations c_{bj} of all the mobile ions are assumed to be constant in bulk solution, wherein the osmotic pressure is given by

$$\Pi_b/k_BT = c_s = \sum_{j^-} c_{jb^-} + \sum_{j^+} c_{jb^+} \tag{14}$$

The distribution of mobile ions obeys the Boltzmann law

$$\frac{c_{j^-}(r)}{c_{jb^-}} = \frac{c_{jb^+}}{c_{j^+}(r)} = \exp[e\Delta\Psi(r)/k_BT] \tag{15}$$

where $\Delta\Psi(r) = \Psi(r) - \Psi_{bulk}$ is excess electrostatic potential in the coronal domain of micelle.

In the framework of LEA, the electrostatic interactions in the corona manifest themselves through the entropy of ions disproportionated between the interior of the corona and bulk solution. Ionic contribution F_{ion} to the coronal free energy F_A is given by

$$F_{ion} = \int_{V_A} f_{ion}(r)\, dV$$

where integration is performed over coronal volume V_A and $f_{ion}(r)$ is the free energy density.

For strong (quenched) PE with constant degree of ionization $\alpha = \alpha_b$

$$\begin{aligned} f_{ion}(r)/k_BT &= \sum_j c_j(r)[\ln c_j(r) - 1] + \Pi_b/k_BT - \sum_j c_{jb} \ln c_{jb} \\ &= c_s\{1 - \sqrt{1 + [\alpha_b c_p(r)/c_s]^2}\} \\ &\quad + \alpha_b c_p(r) \ln\{\alpha_b c_p(r)/c_s + \sqrt{1 + [\alpha_b c_p(r)/c_s]^2}\} \end{aligned} \tag{16}$$

For pH-sensitive PE (weak polyacid), an additional contribution

$$\frac{f_{ionization}(r)}{k_BT} = c_p(r)\left\{\alpha(r)\ln[\alpha(r)] + [1-\alpha(r)]\ln[1-\alpha(r)] - \alpha(r)\ln\frac{K_a}{c_{bH^+}}\right\} \tag{17}$$

accounts for the free energy gain due to ionization of the coronal blocks and leads to

$$\frac{f_{ion}(r)}{k_BT} = c_s\{1 - \sqrt{1 + [\alpha(r)c_p(r)/c_s]^2}\} + c_p(r)\ln[1-\alpha(r)] \tag{18}$$

Here, the degree of ionization $\alpha(r)$ is determined from the equation

$$\frac{\alpha(r)}{1-\alpha(r)}\frac{1-\alpha_b}{\alpha_b} = \sqrt{1 + [\alpha(r)c_p(r)/c_s]^2} - \alpha(r)c_p(r)/c_s \tag{19}$$

where α_b is the degree of ionization of an isolated monomer in the bulk solution at given pH and K_a is the (acidic) dissociation constant. Expansion of eqs 16, 18, and 19 with respect to ratio $\alpha(r)c_p(r)/c_s$ provides asymptotic dependences for f_{ion} in the two limits: $\alpha(r)c_p(r)/c_s \gg 1$ (low salt conditions) and $\alpha(r)c_p(r)/c_s \ll 1$ (high salt conditions). These two regimes are also referred in the literature as osmotic (counterion dominated) and salt dominated regimes of polyelectrolyte brush.[70−72]

At low salt ($\alpha(r)c_p(r)/c_s \gg 1$), the density of the coronal free energy

$$f_{ion}(r)/k_BT \approx \begin{cases} \alpha_b c_p(r)\{\ln[2\alpha_b c_p(r)/c_s] - 1\}, & \text{quenched PE} \\ c_p(r)[-\alpha(r) + \ln(1-\alpha(r))], & \text{annealing PE} \end{cases} \tag{20}$$

and degree of ionization

$$\alpha(r) \approx \begin{cases} \alpha_b, & \text{quenched PE} \\ \{\alpha_b c_s/[2(1-\alpha_b)c_p(r)]\}^{1/2}, & \text{annealing PE} \end{cases} \tag{21}$$

At high salt ($\alpha(r)c_p(r)/c_s \ll 1$), the degree of ionization $\alpha(r)$ approaches the bulk value, $\alpha(r) \approx \alpha_b$, and

$$f_{ion}(r)/k_BT \approx \begin{cases} \alpha_b^2 c_p^2(r)/(2c_s), & \text{quenched PE} \\ \alpha_b^2 c_p^2(r)/(2c_s) + c_p(r)\ln(1-\alpha_b), & \text{annealing PE} \end{cases} \tag{22}$$

In formulation of asymptotic power law dependences for equilibrium parameters of micelles the gradients in polymer density and degree of ionization within corona could be neglected, and $c_p(r)$ and $\alpha(r)$ can be replaced by averaged values, c_p and α. By substituting $c_p(r) \to c_p$ and $\alpha(r) \to \alpha$ in eqs 20, 21, and 22, one finds the electrostatic contribution to the coronal free energy

$$F_{ion} = V_A f_{ion}\{c_p, \alpha\} \tag{23}$$

The scaling models of ionic spherical micelles with strong[62−66] and pH-sensitive PE coronae[67−69] allowed for asymptotic power law dependences of micelle parameters in the limit when short-range nonelectrostatic forces in the corona are negligible compared to long-range electrostatic interactions ($F_A \approx F_{ion}$).

In the osmotic regime, the concentration of counterions in the corona of micelle noticeably exceeds concentration c_s of salt ions in the solution. Under these conditions, differential ion pressure that tends to increase the volume of coronal domain is governed by counterions. By balancing coronal free energy $F_A \approx F_{ion}$ (eqs 23 and 20), with surface contribution $F_{interface}$(eq 2), one finds the parameters of ionic micelle at low salt.

In contrast to the case of a nonionic micelle (eq 6), the aggregation number p in a micelle with strong PE

dx.doi.org/10.1021/ma300195n | Macromolecules XXXX, XXX, XXX−XXX

corona sharply decreases with increasing length of coronal block N_A

$$p \simeq N_B^2 \left(\frac{\gamma_{BS} a^2}{\alpha_b N_A k_B T} \right)^3 \quad (24)$$

Remarkably, eq 24 is valid for both starlike and crew-cut "osmotic" micelles formed by diblock copolymer with strong PE coronal block at low ionic strength.

At low salt concentrations c_s, the entropic penalty for localization of counterions in ionized corona leads to significant increase in critical micelle concentration CMC compared to CMC_n for nonionic micelles

$$\ln \mathrm{CMC} \simeq \frac{\ln \mathrm{CMC}_n}{\alpha_b N_A} \quad (25)$$

An increase in c_s leads to the progressive leveling of the concentrations of co- and counterions in the coronal domain of micelle and in the solution and to the corresponding decrease in differential ion pressure. Simultaneously, local coronal pH approaches that in the bulk solution. At high ionic strength with salt concentration c_s exceeding by far the concentration of ionized monomers in micellar corona, the interactions between charged monomers are screened at distances $r > r_D \simeq (l_B c_s)^{-1/2}$, where r_D is the salt controlled Debye screening length. Here, the difference between pH-sensitive and strong PE block disappears, and the behavior of an ionic micelle resembles that of a micelle with nonionic corona. Electrostatic interactions between coronal monomers are described via an effective salt controlled second virial coefficient $\upsilon_{A,\mathrm{eff}} = (\upsilon_A + \alpha_b^2/2c_s)$, where υ_A is the "bare" excluded volume parameter of coronal monomer unit in the absence of charge (cf. eq 22). In the two limits of starlike and crew-cut micelles, the dependence of aggregation number p on salt concentration c_s is given by

$$p \simeq \begin{cases} (a^2 \gamma_{BS}/k_B T)^{15/11} N_B^{10/11} N_A^{-3/11} (a^{-3} \upsilon_{A,\mathrm{eff}})^{-6/11} \\ \quad \text{starlike micelle} \\ (a^2 \gamma_{BS}/k_B T)^{9/5} N_B^2 N_A^{-9/5} (a^{-3} \upsilon_{A,\mathrm{eff}})^{-6/5} \\ \quad \text{crew-cut micelle} \end{cases} \quad (26)$$

The critical micelle concentration CMC decreases down to CMC_n upon progressive additions of salt ions.

Equation 26 indicates that dependence of micelle hydrodynamic radius on salt concentration c_s should be qualitatively different for starlike and crew-cut aggregates. The overall size of a starlike micelle is determined by extension of the coronal blocks. Two competing trends—crowding of the coronal blocks due to salt-induced increase in p (first line in eq 26) and decreasing binary interactions between monomers $\sim \upsilon_{A,\mathrm{eff}}$ (eq 22)—lead to a slight decrease in micellar size with increasing ionic strength, $R_{\mathrm{micelle}} \approx H \simeq a^{2/5} N_A^{3/5} (p \upsilon_{A,\mathrm{eff}})^{1/5} \sim \upsilon_{A,\mathrm{eff}}^{1/11}$. This theoretical prediction is in reasonable quantitative agreement with experimental findings.[73,83] On the contrary, overall size of a crew-cut micelle is controlled by the radius of micellar core which increases with increasing ionic strength as $R_{\mathrm{micelle}} \approx R \simeq a(N_B p)^{1/3} \sim \upsilon_{A,\mathrm{eff}}^{-2/5}$.

The effect of small additions of salt ions on the behavior of a micelle with pH-sensitive corona could be dramatically different[67,68] from that of a micelle with strong PE corona. In particular, pH-sensitive spherical micelle can undergo sharp transformations triggered by mild variations in solution salinity (at pH $\simeq$ pK) or by variations in pH around pK. Localization of counterions in PE corona gives rise to a locally lower (higher) coronal pH in micelles with polyacidic (polybasic) coronal blocks. As a result, ionization of block A in the corona is lower compared to that in the solution. The coupling between aggregation number p and degree of ionization α of the coronal block could lead to the appearance of two populations of spherical micelles: large ones with weakly ionized corona and small ones with strongly charged corona.[67] In the corona of a large (quasi-neutral) micelle, excluded volume interactions between monomer units dominate over electrostatic ones. Assembly of such deionized aggregate is favored by smaller surface free energy $F_{\mathrm{interface}}$ per chain. In a small charged micelle, the free energy per chain is gained due to ionization of coronal block A. The latter is close to that of a single block A in the bulk solution. A jumplike larger-to-smaller micelle transition occurs when the free energies (per chain) in the large quasi-neutral and small strongly charged micelles become equal. This transition can be triggered by variations in both pH and ionic strength in the solution.

The predicted abrupt micelle transformations were supported by the SCF numerical model[61] and confirmed experimentally.[74] Figure 6 demonstrates the pH-triggered

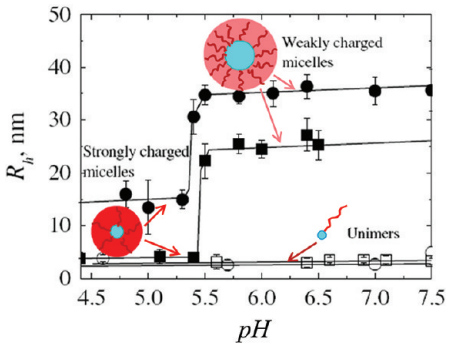

Figure 6. Hydrodynamic radius R_h of micelles formed by $PDMAEMA_{42}$-*b*-$PNIPAM_{52}$ (filled squares) and $PDMAEMA_{57}$-*b*-$PNIPAM_{97}$ (filled circles) and of unimers (open symbols) as a function of solution pH. Subscripts indicate number of monomer units in the corresponding block of copolymer.

rearrangements in spherical micelles of poly(dimethylaminoethyl methacrylate-*block*-poly(*N*-isopropylacrylamide), PDMAEMA-*b*-PNIPAM, block copolymer. In accordance with the theoretical model,[67] an increase in pH leads to deionization of the (polybasic) PDMAEMA coronal block, and the sharp transition from smaller to larger micelles occurs in a narrow interval of pH. We emphasize that such rearrangements are prohibited in spherical micelles with strong PE corona.

Similarly to neutral copolymer micelles, the aggregates formed by asymmetric ionic/hydrophobic block copolymer are capable of changing morphology when they acquire crew-cut shape. The morphological transitions can be triggered by variations in the ionic strength or pH (for pH-sensitive block copolymers) since both factors mediate the strength of repulsive interactions in the coronal domain. Polymorphism in diblock copolymers with ionizable block has the same physical origin as in nonionic copolymers.[75] By comparing free energy increments $\delta F_i = F_{\mathrm{elastic},B} + \Delta F_A$ where $F_{\mathrm{elastic},B}$ is still given by eq 3 while ΔF_A is now specified by both nonionic and electrostatic interactions, one finds the binodals for sphere-to-cylinder and cylinder-to-lamella transitions in ionic aggregates.[30] The values

dx.doi.org/10.1021/ma300195n | *Macromolecules* XXXX, XXX, XXX−XXX

of exponents in the dependences of binodals $N_B^{c-s} \sim N_B^{l-c}$ on the system parameters are different under low and high salt conditions. In particular, at high ionic strength with $\upsilon_{A,eff} \gg \upsilon_A$ the binodal lines corresponding to salt-induced sphere-to-cylinder-to-lamella transitions are given by

$$\frac{\alpha_b^{\,2}}{2c_s a^3} \simeq \frac{N_B^{\,10/9}}{N_A^{\,16/9}}\left(\frac{\gamma_{BS}a^2}{k_BT}\right)^{2/3} \times \{i(i+1)[b_{i+1}(i+1)^2 - b_i i^2]\}^{5/9}, \quad i = 1, 2 \qquad (27)$$

for diblock copolymers with both strongly dissociating and pH-sensitive coronal blocks.[69] (Note that at high ionic strength the degree of ionization α of pH-sensitive block A reaches its maximal value $\alpha = \alpha_b$.)

Under low salt conditions in the osmotic regime, micelles with pH-sensitive corona could demonstrate an unusual ("inverted") sequence of salt induced lamella-to-cylinder-to-sphere morphological transitions (prohibited for micelles with strong PE corona). The binodals for these inverted transitions are specified as[69]

$$\frac{\alpha_b c_s a^3}{1-\alpha_b} \simeq \frac{N_B^{\,2/9}}{N_A^{\,14/9}}\left(\frac{\gamma_{BS}a^2}{k_BT}\right)^{4/3} \times \{i(i+1)[(i+1)^2 b_{i+1} - i^2 b_i]\}^{1/9}, \quad i = 1, 2 \qquad (28)$$

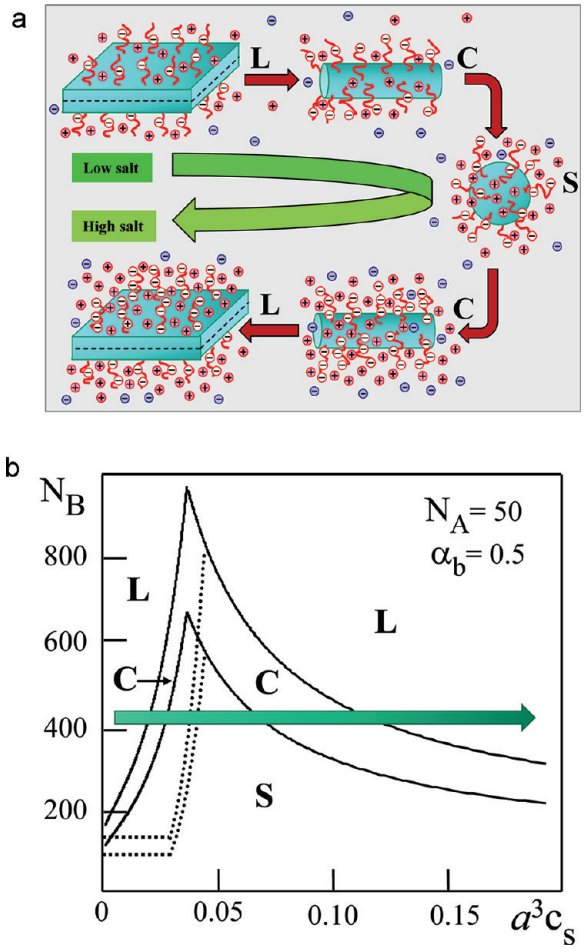

Figure 7. Sequence of salt-induced morphological transitions in diblock copolymer aggregates with pH-sensitive corona (a) and the theoretical diagram of states in N_B, c_s coordinates (b).

The schematic in Figure 7a demonstrates the sequence of morphological transitions for equilibrium aggregates with pH-sensitive corona. In Figure 7b, we present the theoretical diagram of states for block copolymer with short (N_A = 50), pH-sensitive coronal block.[69] Solid lines indicate the binodals calculated with the account of both excluded volume and electrostatic interactions between coronal monomers. Asymptotic dependences calculated with the account for only one type of dominant monomer−monomer interactions (excluded volume or electrostatic ones, eq 28) are indicated by dotted lines. Green arrow marks the intersection of the diagram of states corresponding to the sequence of inverted ($L \rightarrow C \rightarrow S$) and direct ($S \rightarrow C \rightarrow L$) morphological transitions illustrated in Figure 7a.

Recently, a refined semianalytical SCF model[76] has been developed to examine the generic morphologies of micelles with pH-sensitive corona and some novel architectures (branching cylindrical aggregates). The branching cylinders were expected to be thermodynamically stable when the branching (saddle-shaped) segment in a cylindrical micelle has lower free energy than that of the spherical end-caps. The existence of branching architectures has been also proposed for block copolymer with strong PE block in ref 77. However, these structures were not analyzed there in any detail. The effect of polymer concentration on self-assembly of diblock copolymer with strong PE block and on the morphological transitions between aggregates have been also examined.[78]

Theory of micellization of diblock copolymer with non-ionic hydrophilic coronal block A and weakly ionizable (pH-sensitive) hydrophobic coral block B has been developed in ref 79. Weak ionization permitted to maintain the collapsed state of the coral block and to preserve the spherical shape of the micelle. The Poisson−Boltzmann approach allowed for approximate expressions of electrostatic potential $\Psi(x)$ in both coral and coronal domains of the micelle. Although the formalism[79] allowed for a detailed characterization of a micelle with ionizable core and has raised important issues of the system equilibration and polydispersity, no power law dependences for the parameters of such micelles were obtained so far.

To conclude this section, we outline few challenging theoretical problems for micelles with PE corona.

- Comparison between the theoretical predictions for ionic micelles and experiment is often complicated by the arrested molecular exchange between micelles and unimers. The lack of micelle equilibration is attributed to glassy or entanglement dynamics of the core domain or high incompatibility of monomer B and water.[80−82] Efforts have been made to achieve the micelle responsiveness by using copolymers with "soft" hydrophobic block, e.g., poly(isobutylene) linked to pH-sensitive PE block.[83] An alternative strategy to obtain "dynamic" micelles is to induce a certain fraction of ionizable comonomers in the core forming block B. Block copolymers with statistical[84,85] or gradient[86,87] sequences of comonomers in block B linked to pH-responsive block A have demonstrated a reversible pH-controlled association. The aggregation number and dimensions of micelles changed reversibly as a function of the ionic strength and pH in the solution. The assemblies of such block copolymers could be good candidates for quantitative comparison with the theory. However, the theoretical analysis of self-assembly of block copolymer comprising ionizable monomers and comonomers in the associating block is limited,[79] and asymptotic dependences for micelle parameters are lacking.

dx.doi.org/10.1021/ma300195n | Macromolecules XXXX, XXX, XXX−XXX

- Hybrid polypeptide−synthetic block copolymers and amphiphilic block copolypeptides give rise to stimuli-responsive micelles and vesicles.[88−91] The ability of aggregates to change their size and shape due to variations in the solution pH is related to reversible pH induced secondary structure formation in polypeptide blocks. Up to now there is no theory incorporating the effect of secondary structure on association behavior and morphological transitions in pH-responsive peptide-based copolymers.
- A related theoretical problem arises for self-assembled vesicles of amphiphilic copolymer with oligonucleotide-based coronal block.[92] The corona of such vesicle constitutes a "microarray" of single stranded oligonucleotide "probes" that can preferentially hybridize with complementary free DNA fragments ("targets") in the solution. The existing theories focus mostly on hybridization between probes and targets in bulk solution phase and on solid−liquid interfaces such as "DNA chips" (see, e.g., review[93]). The hybridization on self-assembled interface (surface of vesicle) is expected to affect the structure and even morphology of the copolymer aggregate. The analysis of coupling between hybridization and association of the oligonucleotide-based block copolymer presents a challenging theoretical task.
- A number of experimental studies[94,95] demonstrated strong effect of counterion valence on the structure and mechanical properties of PE brushes. While the systems with monovalent salt ions are reasonably well described by the existing theories, di- and trivalent ions lead to a stronger contraction of PE brush than expected from osmotic scaling models.[96] This effect is typically attributed to ion−ion correlations. Clearly, ion valence would also affect the self-assembly of copolymer with PE block. However, up to now the influence of multivalent ions on equilibrium nanostructures with PE coronae was not addressed theoretically.
- The SCF models and existing scaling theories of micelle with ionized corona do not distinguish between intramolecular and intermolecular repulsions between charged coronal monomers. A scaling model of strong starlike PE[97] has accounted for intramolecular electrostatic repulsions within branches and predicted a more complex behavior of such a macromolecule than expected from classical osmotic models. Instead of a single exponent in the power law dependence of polymer size on ionic strength in the salt-dominated regime ($H \sim c_s^{-1/5}$), the revised scaling model[97] predicted several subregimes in salt-induced contraction of the branched PE. Similar modifications could be expected in a micellar corona of any geometry *i*. The impact on self-assembly is jet to be considered.

4. TRIBLOCK CO- AND TERPOLYMER SELF-ASSEMBLY

On scaling level, the self-assembly of linear triblock copolymer *ABA* is similar to that of diblock *AB* with degree of polymerization $N_B/2$ of the core block *B*.[52] In contrast, linear triblock copolymer *BAB* exhibits novel features compared to diblock *AB* with degree of polymerization $N_A/2$ of the coronal block *A*. While in a very dilute solution "flowerlike" micelle with corona consisting of loops *A* resembles its diblock counterpart, an increase in polymer concentration leads to bridging attraction between aggregates and eventual solution gelation.[98] Similarly to spherical micelles, aggregates of cylindrical and lamellar shapes give rise to networks and mesogels[99] where soluble blocks *A* form loops and bridges between condensed cores *B*.

Introduction of the third component *C* makes the behavior of linear terpolymer *ABC* significantly more diverse compared to *AB* or *BC* diblock copolymers. Different solubilities of the three components and the competition to optimize the organization of self-assembling aggregate give rise to a variety of multicompartment micelles (MCMs). A comprehensive discussion of these architectures is presented in recent review.[100] Here, we distinguish between corona- and core-compartmentalized MCMs.

Terpolymers with solvophobic central block *B* and two incompatible solvophilic terminal blocks *A* and *C* give rise to corona-compartmentalized "Janus" micelles. Lateral segregation of soluble blocks *A* and *C* in the corona of Janus micelle has been observed experimentally[101−103] and explored theoretically by means of the two-gradient SCF approach.[104] In an analytical treatment, a loop of block *B* in the core of Janus micelle can be envisioned as composed of two linear chains with length $N_B/2$. To a good approximation, segregation of blocks *A* and *C* in the coronal domain does not affect $F_{B,\text{elastic}}$, and the aggregation number p in Janus micelle can be found by balancing the surface free energy $F_{\text{interface}}$ and the coronal free energy. In the case of nonionic terpolymer with equal lengths of terminal blocks, $N_A = N_C \gg N_B$, and nonselective (athermal) solvent for *A* and *C*, a segregation threshold can be estimated from the blob model of starlike polymer.[26] In a starlike micelle with mixed corona of thickness $H \gg R$ and aggregation number p, each coronal block (*A* or *C*) gives rise to $\simeq p^{1/2} \ln(H/R)$ correlation blobs (eq 5, $i = 3$). Incompatibility of blocks *A* and *C* starts to manifest itself when the interaction free energy due to *A*−*C* contacts $\simeq k_B T \chi_{AC} p^{1/2} \ln(H/R)$ becomes on the order of the thermal energy or, equivalently, when $\chi_{AC} \sim p^{-1/2}(\ln N_A)^{-1}$ with $p \sim N_B^{4/5}$ given by eq 6. Above segregation threshold, separation of blocks *A* and *C* into distinct domains gives rise to additional *A*/*C* interfaces within micellar corona and associated free energy losses. However, the free energy increase due to *A*/*C* interfaces remains smaller than the dominant coronal contribution $\sim k_B T p^{3/2}$. Therefore, the power law asymptotic dependence for aggregation number p (eq 6) does not change in a starlike Janus micelle with segregated corona. For weakly incompatible blocks *A* and *C*, the coronal segregation occurs via formation of several *A*- and *C*-rich coronal domains of diverse and strongly fluctuating geometries. The segregation into two hemispheres, *A* and *C*, with sharp interface could be triggered by application of the external field or by adsorption of micelles at liquid−liquid interface.

Core-compartmentalized MCMs of diverse morphologies (e.g., core−shell spheres,[101,105] spherical aggregates with "hamburger", "clover" or "football" cores,[100,106,107] core−shell or core segmented cylinders,[100,106,108,109] etc.) are formed by terpolymers with one soluble and two insoluble blocks.

Microsegregation of the MCM core into domains comprising different components makes the theoretical evaluation of the free energy per chain in such an aggregate significantly more complicated than in a diblock copolymer micelle. Approximation of the domain shape by lens[110] or spherical segment[106] allows for a reasonable simplification of the MCM model. For example, when terpolymer comprising two insoluble components (*B* and *C*) is asymmetric in composition ($N_B \ll N_C$), a starlike MCM has a "football" core. The surface free energy $F_{\text{interface}}$ in such a micelle can be represented as a function of number n of domains *B* (modeled as spherical segments) on the surface of core *C*. By ignoring the confinement free energies of blocks *B* and *C*, and decomposing the corona of soluble blocks *A* into n spherical sub-brushes adjacent to domains *B*,

dx.doi.org/10.1021/ma300195n | Macromolecules XXXX, XXX, XXX−XXX

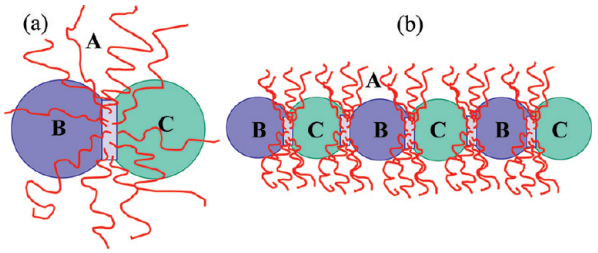

Figure 8. Schematic of 3-miktoarm terpolymer micelles with dumble-like (a) and segmented cylindrical core (b).

and a laterally homogeneous sub-brush at larger distances, one can formulate the free energy per chain in such MCM as a function of number of compartments n, aggregation number p, surface tensions γ_{BS} and γ_{CS} at the core−corona boundary, surface tension γ_{BC} at the interface between B and C domains, and molecular weights of the blocks, N_A, N_B, and N_C. Minimization of the free energy with respect to n and p allows for power law dependences for the MCM parameters. With accuracy of the logarithmic prefactor, the number n of compartments in a starlike MCM with "football" core is estimated as[106]

$$n \simeq \left(\frac{N_C}{N_B}\right)^{4/5}\left(\frac{\gamma_{CS}}{\tilde{\gamma}_{BS}}\right)^{6/5} \tag{29}$$

As it follows from eq 29, the number of compartments n increases with an increase in terpolymer asymmetry, N_C/N_B, and can be also tuned by variations in the free energy of core−corona interface. Here, $\tilde{\gamma}_{BS} \simeq \gamma_{BS}(1 - \cos\theta)^{2/3}(1 + 0.5\cos\theta)^{1/3}$, and $\theta = \arccos[(\gamma_{CS} - \gamma_{BC})/\gamma_{BS}]$ is the contact angle. This theoretical prediction is in a good qualitative agreement with recent experimental observations.[106]

However, neglecting the confinement free energy of core blocks is not granted for arbitrary terpolymer composition. It is reasonable to assume that, similarly to generic morphologies of diblock copolymer, the geometry of a crew-cut terpolymer aggregate in a dilute solution is dictated by the free energy increment, $\delta F = F_{B,\mathrm{elastic}} + F_{C,\mathrm{elastic}} + \Delta F_A$, where now all the three contributions, $F_{B,\mathrm{elastic}}$, $F_{C,\mathrm{elastic}}$, and ΔF_A depend on internal organization of the MCM core (e.g., number and shape of the core compartments). A precise formulation of δF and description of MCM parameters and morphology as a function of molecular weights and solubilities of components A, B, and C constitute a set of challenging problems for future theoretical studies.

Changing terpolymer architecture from linear to 3-miktoarm star leads to a number of novel self-assembled structures.[111−113] The theoretical studies on 3-miktoarm terpolymer[114−117] focused mostly on the analysis of morphologies (lamella, polygonal cylinders, perforated layer, lamella-in-sphere, etc.) in a melt state. Computer simulation of such systems[117] demonstrated that in all these phases junctions between the blocks in 3-miktoarm terpolymer localize on lines where three interfaces A/B, A/C, and B/C merge. Monte Carlo simulations in a dilute solution[118] indicated the presence of spherical micelles with dumble-like core and modulated core segmented cylinders for 3-miktoarm terpolymer with two insoluble blocks (see Figure 8). A scaling model[119] adopts simplifying approximations to describe confinement of the chains in a dumble-like core and allows for power law asymptotic dependences for micelle parameters only in certain limits. A comprehensive theoretical modeling of such architectures at arbitrary compositions and solubilities of the terpolymer components is currently lacking.

5. CONCLUSIONS

We have reviewed recent developments in the theory of self-assembly of flexible solvophobic/solvophilic diblock copolymer in a dilute solution. In our opinion, an analytical theory of non-ionic diblock copolymer micelles is now developed to a level sufficient for a detailed quantitative comparison with experiment. The theory of ionic micelles with PE coronae is less developed. Here, a basic description of self-assembled aggregates is achieved mostly on the level of asymptotic power law dependences or numerical modeling. The analytical developments are limited to simplified models of coronal charge and ion distributions and linear elasticity of PE coronal chains. The theory of triblock terpolymer self-assembly is largely underdeveloped and constitutes a challenging set of problems.

AUTHOR INFORMATION

Notes

The authors declare no competing financial interest.

Biographies

Ekaterina Zhulina received S.M. in molecular biophysics (with honors) from Leningrad State University in 1975. She earned her Ph.D. in polymer physics in 1981 from the Institute of Macromolecular Compounds of the Russian Academy of Sciences, working with Professor T. M. Birshtein and Dr. A. M. Skvortsov. In 1989, she was awarded Doctor of Sciences Degree in physics and mechanics of polymers for developing the statistical theory of complex macromolecular systems and promoted to Senior Researcher. She became a Leading Research Fellow at the Institute of Macromolecular Compounds of the Russian Academy of Sciences in 1992. As visiting scientist, Ekaterina Zhulina performed research at Max Plank Institute for Polymer Research and Johannes Gutenberg University in Germany, DRFMC-CEA and Joseph Fourier University in France, Wageningen University in The Netherlands, University of North Carolina and University of Texas in the USA, etc. Ekaterina has authored or coauthored over 160 papers in the field of polymer science. Her research interests include the self-assembly of macromolecules in solutions and at interfaces, conformational transitions,

dx.doi.org/10.1021/ma300195n | Macromolecules XXXX, XXX, XXX−XXX

interpolyelectrolyte complexes, and ionizable and biological polymer brushes.

Oleg Borisov was born in Leningrag (now St. Petersburg), Russia, and graduated from Department of Physics and Mechanics of Leningrad Polytechnical Institute. He has received his PhD in physics and mechanics of polymers under the direction of T. M. Birshtein in the Institute of Macromolecular Compounds of the Russia Academy of Sciences, where he worked as a senior researcher since 1991. In 2007, he has joined as a research director the Interdisciplinary Institute of Environmental and Material Research (IPREM) in Pau, France. O. Borisov has received the Friedrich Wilhelm Bessel Research Award (2004) from the Alexander von Humboldt Foundation. His research interests are focused on theory and modeling of polymeric systems of complex architectures in solutions and at interfaces.

■ ACKNOWLEDGMENTS

Partial financial support from the Russian Foundation for Basic Research (RFBR grant 11-03-00969-a) and from the Scientific and Technological Cooperation Program Switzerland-Russia project "Experimental studies and theoretical modeling of amphiphilic di/triblock and dendritic functional polymers at surfaces: influence of interfacial architecture on biological response" (Grant Agreement 128308) is acknowledged.

■ REFERENCES

(1) Riess, G. *Prog. Polym. Sci.* **2003**, *28*, 1107.
(2) Quémener, D.; Deratani, A.; Lecommandoux, S. *Top. Curr. Chem.* **2012**, *322*, 165.
(3) Meier, D. J. *J. Polym. Sci., Part C* **1969**, *26*, 81.
(4) Helfand, E.; Tagami, Y. *J. Chem. Phys.* **1972**, *56*, 3592; *57*, 1812.
(5) Helfand, E.; Wasserman, Z. R. *Macromolecules* **1976**, *9*, 879; **1978**, *11*, 960; **1980**, *13*, 994.
(6) Noolandi, J.; Hong, K. M. *Macromolecules* **1983**, *16*, 1443.
(7) Leibler, L.; Orland, H.; Wheeler, J. C. *J. Chem. Phys.* **1983**, *79*, 3550.
(8) Leermakers, F. A. M.; Scheutjens, J. M. H. M. *J. Chem. Phys.* **1988**, *89*, 3264.
(9) Yuan, X.-F.; Masters, A. J.; Price, C. *Macromolecules* **1992**, *25*, 6876.
(10) Fleer, G. J.; Cohen Stuart, M. A.; Scheutjens, J. M. H. M.; Cosgrove, T.; Vincent, B. *Polymers at Interfaces*; Chapman & Hall: London, 1993.
(11) Leermakers, F. A. M.; Eriksson, J. C.; Lyklema, J. In *Fundamentals of Interface and Colloid Science*; Lyklema, J., Ed.; Elsevier: Amsterdam, 2005; Vol. *V*, p 4.1.
(12) Edwards, S. F. *Proc. Phys. Soc.* **1965**, *85*, 613.
(13) Flory, P. *Principles of Polymer Chemistry*; Cornell University Press: Ithaca, NY, 1953.
(14) Kik, R. A.; Lermakers, F. A. M.; Kleijn, J. M. *Phys. Chem. Chem. Phys.* **2005**, *7*, 1996; *Phys. Rev. E* **2010**, *81*, 021915.
(15) Shi, A.-C.; Noolandi, J. *Macromol. Theory Simul.* **1999**, *8*, 214.
(16) Wang, Q.; Taniguchi, T.; Fredrickson, G. H. *J. Phys. Chem. B* **2004**, *108*, 6733.
(17) de Gennes, P.-J. *Scaling Concepts in Polymer Physics*; Cornell University Press: Ithaca, NY, 1979.
(18) Birshtein, T. M. *Polym. Sci. USSR* **1982**, *A24*, 2110.
(19) Schaefer, D. W.; Joanny, J.-F.; Pincus, P. *Macromolecules* **1980**, *13*, 1280.
(20) de Gennes, P.-J. In *Solid State Physics*; Academic Press: NewYork, 1978; p 1.
(21) Zhulina, Y. B.; Birshtein, T. M. *Polym. Sci. USSR* **1985**, *27*, 570.
(22) Birshtein, T. M.; Zhulina, E. B. *Polymer* **1989**, *30*, 170.
(23) Halperin, A. *Macromolecules* **1987**, *20*, 2943.
(24) Alexander, S. *J. Phys. (Paris)* **1977**, *38*, 983.
(25) de Gennes, P.-J. *Macromolecules* **1980**, *13*, 1069.
(26) Daoud, M.; Cotton, J. P. *J. Phys. (Paris)* **1982**, *43*, 531.
(27) Birshtein, T. M.; Zhulina, E. B. *Polymer* **1984**, *25*, 1453.
(28) Semenov, A. N. *Sov. Phys. JETP* **1985**, *61*, 733.
(29) Zhulina, E. B.; Adam, M.; Sheiko, S.; LaRue, I.; Rubinstein, M. *Macromolecules* **2005**, *38*, 5330.
(30) Borisov, O. V.; Zhulina, E. B.; Leermakers, F. A. M.; Müller, A. H. E. *Adv. Polym. Sci.* **2011**, *241*, 1.
(31) Willner, L.; Poppe, A.; Allgaier, J.; Monkenbusch, M.; Lindner, P.; Richter, D. *Europhys. Lett.* **2000**, *51*, 628.
(32) Jensen, G. V.; Shi, Q.; Hernansanz, M. J.; Oliveira, C. L. P.; Deen, G. R.; Almdal, K.; Pederson, J. S. *J. Appl. Crystallogr.* **2011**, *44*, 473.
(33) Förster, S.; Zisenis, M.; Wenz, E.; Antonietti, M. *J. Chem. Phys.* **1996**, *104*, 9956.
(34) Zhulina, E. B.; Birshtein, T. M.; Borisov, O. V. *Eur. Phys. J. E* **2006**, *20*, 243.
(35) Birshtein, T.; Lyatskaya, Yu. *Macromolecules* **1994**, *27*, 1256.
(36) Lai, P.-Y.; Halperin, A. *Macromolecules* **1992**, *25*, 6693.
(37) Birshtein, T. M.; Zhulina, E. B.; Merkurieva, A. A. *Macromol. Theory Simul.* **2000**, *9*, 47.
(38) Merkurieva, A. A.; Leermakers, F. A. M.; Birshtein, T. M.; Fleer, G. L.; Zhulina, E. B. *Macromolecules* **2000**, *33*, 1072.
(39) Nagarajan, R.; Ganesh, K. *Macromolecules* **1989**, *22*, 4312.
(40) Cogan, K. A.; Leermakers, F. A. M.; Gast, A. P. *Langmuir* **1992**, *8*, 429.
(41) MacEvan, S. R.; Chilkoti, A. *Pept. Sci.* **2010**, *94*, 60.
(42) Dreher, M. R.; Simnick, A. J.; Fischer, K.; Smith, R. J.; Patel, A.; Schmidt, M.; Chilkoti, A. *J. Am. Chem. Soc.* **2008**, *130*, 687.
(43) Trent, A.; Marullo, R.; Lin, B.; Black, M.; Tirrell, M. *Soft Matter* **2011**, *7*, 9572.
(44) Kastantin, M.; Tirrell, M. *Macromolecules* **2011**, *44*, 4977.
(45) Gervais, M.; Gallot, B. *Makromol. Chem.* **1973**, *171*, 157.
(46) Lin, E. K.; Gast, A. P. *Macromolecules* **1996**, *29*, 4432.
(47) Yin, L.; Hillmyer, M. A. *Macromolecules* **2011**, *44*, 3021.
(48) Schmalz, H.; Schmelz, J.; Drechsler, M.; Yuan, J.; Walther, A.; Schweimer, K.; Mihut, A. *Macromolecules* **2008**, *41*, 3235.
(49) Schmelz, J.; Karg, M.; Hellweg, T.; Schmalz, H. *ACS Nano* **2011**, *5*, 9523.
(50) Yu-Su, S. Y.; Sheiko, S. S.; Lee, H.-I.; Jakubowski, W.; Nese, A.; Matyjaszewski, K.; Anokhin, D.; Ivanov, D. A. *Macromolecules* **2009**, *42*, 9008.

(51) DiMarzio, E. A.; Guttman, C. M.; Hoffman, J. D. *Macromolecules* **1980**, *13*, 1194.
(52) Birshtein, T. M.; Zhulina, E. B. *Polymer* **1990**, *31*, 1312.
(53) Zhang, L.; Eisenberg, A. *Science* **1995**, *268*, 1724.
(54) Zhang, L.; Eisenberg, A. *J. Am. Chem. Soc.* **1996**, *118*, 3168.
(55) Zhang, L.; Barlow, R. J.; Eisenberg, A. *Macromolecules* **1995**, *28*, 6055.
(56) Manning, G. *J. Chem. Phys.* **1969**, *51*, 3249.
(57) Borisov, O. V.; Zhulina, E. B.; Leermakers, F. A. M.; Ballauff, M.; Müller, A. H. E. *Adv. Polym. Sci.* **2011**, *241*, 57.
(58) Zhulina, E. B.; Borisov, O. V. *J. Chem. Phys.* **1997**, *107*, 5952.
(59) Zhulina, E. B.; Borisov, O. V. *Langmuir* **2011**, *27*, 10615.
(60) Tamashiro, M. N.; Hernández-Zapata, E.; Schorr, P. A.; Balastre, M.; Tirrell, M.; Pincus, P. *J. Chem. Phys.* **2001**, *115*, 1960.
(61) Lauw, Y.; Leermakers, F. A. M.; Cohen Stuart, M. A.; Borisov, O. V.; Zhulina, E. B. *Macromolecules* **2006**, *39*, 3628.
(62) Marko, J. F.; Rabin, Y. *Macromolecules* **1992**, *25*, 1503.
(63) Wittmer, J.; Joanny, J.-F. *Macromolecules* **1993**, *26*, 2691.
(64) Shusharina, N. P.; Nyrkova, I. A.; Khokhlov, A. R. *Macromolecules* **1996**, *29*, 3167.
(65) Dan, N.; Tirrell, M. *Macromolecules* **1993**, *26*, 4310.
(66) Borisov, O. V.; Zhulina, E. B. *Macromolecules* **2002**, *35*, 4472.
(67) Zhulina, E. B.; Borisov, O. V. *Macromolecules* **2002**, *35*, 9191.
(68) Borisov, O. V.; Zhulina, E. B. *Langmuir* **2005**, *21*, 3229.
(69) Zhulina, E. B.; Borisov, O. V. *Macromolecules* **2005**, *38*, 6726.
(70) Pincus, P. A. *Macromolecules* **1991**, *24*, 2912.
(71) Borisov, O. V.; Birshtein, T. M.; Zhulina, E. B. *J. Phys. II* **1991**, *1*, 521.
(72) Borisov, O. V.; Zhulina, E. B.; Birshtein, T. M. *Macromolecules* **1994**, *27*, 4795.
(73) Föerster, S.; Hemsdorf, N.; Böttcher, C.; Lindner, P. *Macromolecules* **2002**, *35*, 4096.
(74) Xu, L.; Zhu, Z.; Borisov, O. V.; Zhulina, E. B.; Sukhishvili, S. A. *Phys. Rev. Lett.* **2009**, *103*, N118301.
(75) Borisov, O. V.; Zhulina, E. B. *Macromolecules* **2003**, *36*, 10029.
(76) Victorov, A. I.; Plotnikov, N. V.; Hong, P.-G. *J. Phys. Chem. B* **2010**, *114*, 8846.
(77) Netz, R. R. *Europhys. Lett.* **1999**, *47*, 391.
(78) Venev, S. V.; Reineker, P.; Potemkin, I. I. *Macromolecules* **2010**, *43*, 10735.
(79) Nyrkova, I.; Semenov, A. N. *Faraday Discuss.* **2005**, *128*, 113.
(80) Munk, P.; Ramieddi, C.; Tian, M.; Webber, S. E.; Prochazka, K.; Tuzar, Z. *Macromol. Chem., Macromol. Symp.* **1992**, *58*, 195.
(81) Rager, T.; Meyer, W. H.; Wegner, G. *Macromol. Chem. Phys.* **1999**, *200*, 1672.
(82) Won, Y.-Y.; Davis, H. T.; Bates, F. S. *Macromolecules* **2003**, *36*, 953.
(83) Burkhardt, M.; Martinez-Castro, N.; Tea, S.; Drechsler, M.; Babin, I.; Grishagin, I.; Schweins, R.; Pergushov, D. V.; Gradzielski, M.; Zezin, A. B.; Müller, A. H. E. *Langmuir* **2007**, *23*, 12864.
(84) Lejeune, E.; Drechsler, M.; Jestin, J.; Müller, A. H. E.; Chassenieux, C.; Colombani, O. *Macromolecules* **2010**, *43*, 2667.
(85) Charbonneau, C.; Chassenieux, C.; Colombani, O.; Nicolai, T. *Macromolecules* **2011**, *44*, 4487.
(86) Borisova, O. V.; Billon, L.; Zaremski, M.; Grassl, B.; Bakaeva, Z.; Lapp, A.; Stepanek, P.; Borisov, O. V. *Soft Matter* **2011**, *7*, 10824.
(87) Borisova, O. V.; Billon, L.; Zaremski, M.; Grassl, B.; Bakaeva, Z.; Lapp, A.; Stepanek, P.; Borisov, O. V. *Soft Matter.*, submitted for publication.
(88) Carlsen, A.; Lecommandoux, S. *Curr. Opin. Colloid Interface Sci.* **2009**, *14*, 329.
(89) Checot, F.; Rodriguez-Hernandez, J.; Gnanou, Y.; Lecommandoux, S. *Biomed. Eng.* **2007**, *24*, 81.
(90) Checot, F.; Brulet, A.; Oberdisse, J.; Gnanou, Y.; Mondain-Monval, O.; Lecommandoux, S. *Langmuir* **2005**, *21*, 4308.
(91) Tirrell, M. *AIChE J.* **2005**, *51*, 2386.
(92) Teixeira, F.; Rigler, P.; Vebert-Nardin, C. *Chem. Commun.* **2007**, *11*, 1130.
(93) Halperin, A.; Buhot, A.; Zhulina, E. B. *J. Phys.: Condens. Matter* **2006**, *18*, 463.
(94) Konradi, R.; Rühe, J. *Macromolecules* **2005**, *38*, 4345.
(95) Li, F. Polyelectrolyte Brushes at Interfaces: Properties, Structure and Interactions. PhD Thesis, University of California at Santa Barbra, 2005
(96) Birshtein, T. M.; Zhulina, E. B. *Ber. Bunsen-Ges. Phys. Chem.* **1996**, *100*, 929. Zhulina, E. B.; Borisov, O. V.; Birshtein, T. M. *Macromolecules* **1999**, *32*, 8189.
(97) Shusharina, N. A.; Rubinstein, M. *Macromolecules* **2008**, *41*, 203.
(98) Semenov, A. M.; Joanny, J.-F.; Khokhlov, A. R. *Macromolecules* **1995**, *28*, 1066.
(99) Halperin, A.; Zhulina, E. B. *Prog. Coll. Polym. Sci.* **1992**, *90*, 156.
(100) Moughton, A. O.; Hillmyer, M. A.; Lodge, T. P. *Macromolecules* **2012**, *45*, 2.
(101) Erhardt, R.; Zhang, M.; Böker, A.; Zettl, H.; Abetz, C.; Frederik, P.; Krausch, G.; Abetz, V.; Müller, A. H. E. *J. Am. Chem. Soc.* **2003**, *125*, 3260.
(102) Walther, A.; Müller, A. H. E. *Soft Matter* **2008**, *4*, 663.
(103) Walther, A.; Barner-Kowollik, C.; Müller, A. H. E. *Langmuir* **2010**, *26*, 12237.
(104) Charlaganov, M. I.; Borisov, O. V.; Leermakers, F. A. M. *Macromolecules* **2008**, *41*, 3668.
(105) Bütün, V.; Wang, X.-S.; de Paz Báñez, M. V.; Robinson, K. L.; Billingham, N. C.; Armes, S. P.; Tuzar, Z. *Macromolecules* **2000**, *33*, 1.
(106) Gröschel1, A. H.; Schacher, F. H.; Schmalz, H.; Borisov, O. V.; Zhulina, E. B.; Walther, A.; Müller, A. H. E. *Nat. Commun.* **2012**, *3*, 710.
(107) Laschewsky, A. *Curr. Opin. Colloid Interface Sci.* **2003**, *8*, 274.
(108) Liu, Y.; Abetz, V.; Müller, A. H. E. *Macromolecules* **2003**, *36*, 7894.
(109) Stewart, S.; Liu, G. *Angew. Chem., Int. Ed.* **2000**, *39*, 340.
(110) Holmes, R. M.; Williams, D. R. M. *Macromolecules* **2011**, *44*, 6172.
(111) Li, Z.; Hillmyer, M. A.; Lodge, T. P. *Langmuir* **2006**, *22*, 9409.
(112) Saito, N.; Liu, C.; Lodge, T. P.; Hillmyer, M. A. *ACS Nano* **2010**, *4*, 1907.
(113) Li, Z.; Kesselman, E.; Talmon, Y.; Hillmyer, M. A.; Lodge, T. P. *Science* **2004**, *306*, 98.
(114) He, X. H.; Huang, L.; Liong, H. J.; et al. *J. Chem. Phys.* **2002**, *116*, 10508.
(115) He, X. H.; Huang, L.; Liong, H. J.; Pan, C. *J. Chem. Phys.* **2003**, *118*, 9861.
(116) Birshtein, T. M.; Polotsky, A.; Abetz, V. *Macromol. Theory Simul.* **2004**, *13*, 512.
(117) Gemma, T.; Hatono, A.; Dotera, T. *Macromolecules* **2002**, *35*, 3225.
(118) Zhu, Y.; Li, R. K. Y.; Jiang, W. *Chem. Phys.* **2006**, *327*, 137.
(119) Zhulina, E. B.; Borisov, O. V. *Macromolecules* **2008**, *41*, 5934.